Chalcogenide Letters Vol. 17, No. 2, February 2020, p. 41 - 47

# STRUCTURE OF $Ge_2Sb_2Te_5$ THIN FILMS NEAR THE INFLECTION POINT OF THE RESISTIVITY TEMPERATURE DEPENDENCE

Y. ZAYTSEVA[a,*], P. LAZARENKO[a], YU. VOROBYOV[b], A. YAKUBOV[a], N. BORGARDT[a], S. KOZYUKHIN[c,d], A. SHERCHENKOV[a]
[a]*National Research University of Electronic Technology, Zelenograd 124498, Russia*
[b]*Ryazan State Radio Engineering University, Ryazan 390005, Russia*
[c]*Kurnakov Institute of General and Inorganic Chemistry, RAS, Moscow 119991, Russia*
[d]*National Research Tomsk State University, Tomsk, 634050, Russia*

We investigated $Ge_2Sb_2Te_5$ thin films annealed at the temperatures specific to the crystallization process using transmission electron microscopy. The annealing temperatures typical for the inflection point (168 °C) of the temperature dependence of resistivity and at the end of the crystallization process (183 °C) were chosen for the TEM studies. These studies clearly showed that the inflection point on the temperature dependence of resistivity is identified with a two-stage character of $Ge_2Sb_2Te_5$ thin films crystallization.

(Received October 01, 2019; Accepted February 3, 2020)

*Keywords*: $Ge_2Sb_2Te_5$, Phase change material, Thin film, Crystallization, Resistivity, Inflection point, Transmission electron microscopy

## 1. Introduction

Chalcogenide phase change materials (PCM), such as Ge-Sb-Te (GST) alloys, are of high interest due to their successful commercial application. The advantage of GST materials is a variety of phase states (amorphous and different crystalline) with various physical and chemical properties, the fast and reversible transition between which underlies the operation principle of PCM based devices [1,2].

GST materials are widely used as rewritable storage media. Currently, a new type of non-volatile memory is developing, that will allow multi-level storage in a cell using intermediate phases between fully crystalline and fully amorphous states [3,4]. Also, GST alloys are very attractive for configurable photonic applications such as phase change optical metamaterials, metasurfaces and optoelectronic displays [5-7].

The crystallization process is considered to be the slowest operation of the PCM work, thus limiting the overall performance of the PCM devices [8]. That is why improving PCM technology requires detailed knowledge of the crystallization kinetics in thin GST films. The crystallization process was studied in detail using various methods, including transmission electron microscopy (TEM) [9-11]. It was found that as-deposited amorphous thin films crystallize into a metastable phase with a NaCl-type structure (*Fm-3m*) [12] and then transform into a stable hexagonal structure (*P-3m1*) [13]. In various researches, the crystallization process is initiated by laser irradiation, heating, electrical current and other ways. In our study, we focused on thermal crystallization, currently studied extensively. However, the crystallization mechanism and, in particular, the parameters of nucleation and grain growth, are still not well understood and under discussion [10,11,14].

One of the common methods for studying the dynamics of the crystallization process in GST is in situ measurement of resistivity during heating. This is primarily due to the fact that the

* Corresponding author: julia3ybina@gmail.com

resistivity of GST thin films significantly decreases (by three orders of magnitude or more) during the crystallization process. The presence of phase states with different conductivities in the GST material makes it attractive for multilevel memory devices. For this purpose, it is necessary to control the crystallization process precisely. However, our experimental data and result of the literature analysis show that the resistivity variation during the crystallization process is not simple. Our attention is attracted to the point of inflection on the resistivity temperature dependence during crystallization that was observed in some works [15-20]. This may indicate a multistage character of the crystallization process in GST. TEM provides great opportunities for an analysis of the GST structure formed near the inflection point, which is necessary for the understanding of this effect.

One of the models explaining the process of electrical switching in chalcogenide PCM is based on the hypothesis of the formation of a percolation path and a current filament in the case of a high electric field [21]. This channel is formed from conductive crystalline regions, respectively, it can be assumed that the inflection point is associated with the formation of percolation channels also. Since TEM provides great opportunities for the structural analysis, we used this method for estimating the possible formation of crystalline conductivity channels near the inflection point.

So, in this paper, we performed TEM studies of the $Ge_2Sb_2Te_5$ films annealed at temperatures near the inflection of the resistivity temperature dependence during crystallization. The obtained results are compared with electrophysical measurements.

## 2. Experimental

Thin films of the GST composition were prepared by DC magnetron sputtering at room temperature. The pressure of Ar during the process was $5 \cdot 10^{-3}$ Torr, the sputtering power was 100 W. The thin films were deposited on the thermally oxidized silicon substrates with planar electrodes (TiN/W/TiN). The thicknesses of deposited thin films were ~130 nm.

The transmission electron microscopy experiments were carried out on an FEI Titan Themis 200-80 microscope operated at 200 kV and equipped with an objective lens spherical aberration corrector and energy dispersive X-ray (EDX) spectrometer Super-X. Cross section TEM specimens were prepared by the standard in-situ lift-out technique [22] on FEI Helios NanoLab 650 dual-beam workstation equipped with Kleindiek MM3A-EM micromanipulator. The elements distribution across the prepared cross section specimen of the as-deposited thin film was determined by EDX. The heating stage (HFS600E-PB4 Linkam), containing the silver hot-plate and platinum thin film sensor, with a temperature controller (T95-STD Linkam) were used for the annealing of the as-deposited thin films. The specific annealing temperatures were chosen near the inflection of the resistivity temperature dependence during crystallization. The annealing was carried out at constant heating and cooling rates of 5 °C/min under argon atmosphere. Multimeter Keithley 2002 and picoammeter Keithley 6485 were used for controlling the temperature resistivity dependencies of samples during annealing.

The structures of as-deposited and annealed $Ge_2Sb_2Te_5$ thin films were studied by means of electron diffraction and high-resolution (HR) TEM images analysis.

## 3. Results and discussion

TEM studies showed that as-deposited $Ge_2Sb_2Te_5$ film has a uniform thickness of about 130 nm. To study the structure of the film, a selected area diffraction pattern (SAED) was obtained, as shown by the dashed circle in Fig. 1a. According to the SAED data, the as-deposited thin film was amorphous (Fig. 1b). Two peaks on the radial intensity profile formed on the basis of experimental diffraction data correspond to the 3.12 and 1.95 Å, which is in agreement with the literature data for the amorphous GST material [23,24]. Results of the EDX proved that the distribution of elements across the film is uniform and composition of the as-deposited thin film is close to $Ge_2Sb_2Te_5$ (Fig. 1c).

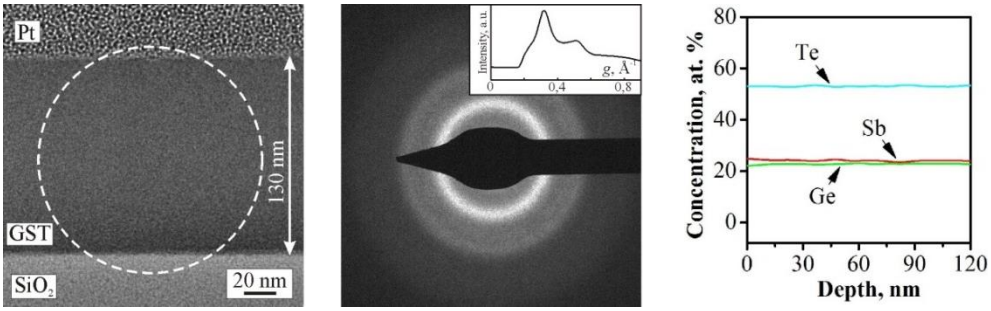


*a)* *b)* *c)*

*Fig. 1. TEM image of the as-deposited GST film (a) with a white dashed circle indicating the area from which the electron diffraction data were obtained (b), the elemental distribution of the as-deposited film across the thickness determined by X-ray microanalysis using TEM (c).*

Fig. 2 shows the temperature dependence of resistivity for as-deposited $Ge_2Sb_2Te_5$ thin film obtained during heating to 400 °C and subsequent cooling. The initial film in the range from room temperature to about 150 °C has an exponential dependence of resistivity, which is typical for the amorphous state [25] and correlates with the results of electron diffraction. Further heating above 150 ºC leads to a significant decrease in resistivity that ends at about 185 ºC. The crystallization of investigated thin film into the NaCl structure can explain this decrease [26]. The next drop in resistance, corresponding to the transition into a stable hexagonal structure [27], is observed in the temperature range from 325 to 375 ºC.

Analysis of the crystallization temperature range allows identifying the three regions with different dependencies of resistivity (see Fig. 2). The first region is a sharp decrease in resistivity for $Ge_2Sb_2Te_5$ thin film in the range from 160 to 168 °C. The second region corresponds to the curve inflection of the resistivity temperature dependence that also was observed in the number of works [15-20]. The third region in the temperature range from 175 to 183 °C is accompanied by the end of the decrease in resistivity. These regions and inflection of the resistivity temperature dependence indicate a multistage character of the crystallization process. So, specific annealing temperatures (168 and 183 °C) were chosen in the range of significant decrease in resistivity, which is due to the phase transition from the initial amorphous to the crystalline phase.

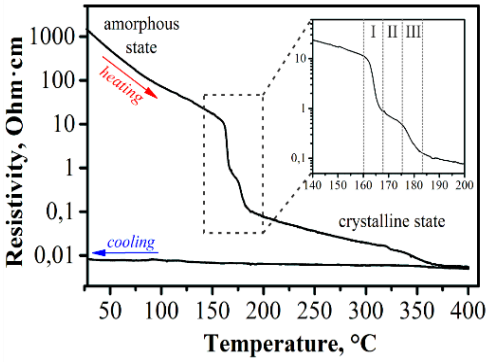


*Fig. 2. The temperature dependence of resistivity for the $Ge_2Sb_2Te_5$ thin film.*

As follows from our measurement, the GST film resistance decreases by an order of magnitude upon annealing to 168 ºC (Fig. 3a). Interestingly, in general, the film structure remains amorphous, as it is shown in the SAED pattern in Fig. 3b. Two intensity peaks correspond to 3.11 and 1.92 Å, which coincides with the typical values for amorphous GST. However, detailed high-resolution TEM images analysis shows the presence of GST crystallites, the size of which does not exceed 7 nm in the cross section of the TEM specimen. The observed crystallites have a cubic

phase with fcc lattice and are distributed along the film thickness in a random way. As an example, the inset in Fig. 3c shows a zoomed fragment of high-resolution TEM image illustrating the GST grain in [100] zone axis. The fraction of the crystalline phase in the plane of the sample cross section was estimated by means of HRTEM images analysis and amounted to less than 2 percent. The fact that such GST grains were not observed in the as-deposited film allows to conclude that crystallites were formed during the annealing, but not under the influence of an electron beam in the electron microscope.

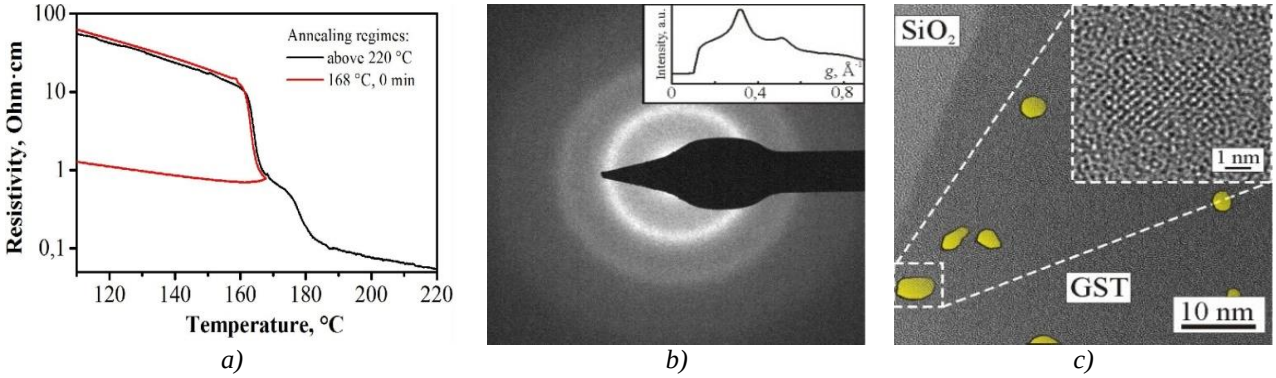


*Fig. 3. The temperature dependence of resistivity (a), SAED pattern (b) and HRTEM image with GST crystallites highlighted in yellow color for the sample after annealing at 168 °C. Zoomed fragment with GST grain is shown in the inset (c)*

Apparently, crystallization of the investigated thin films started from the formation of crystalline nuclei in the film volume. However, even though the detected fraction of crystalline material was practically negligible, change in the material resistivity, on the other hand, was above one order of magnitude. Effective medium approximation theory [28] cannot predict such a drastic change even in spite of the fact that the difference between resistivity values of amorphous and crystalline $Ge_2Sb_2Te_5$ films can reach several orders of magnitude. Another mechanism of the conductivity increase should be involved and more detail investigations are needed in order to reveal the influence of small crystallites on the electrical properties of $Ge_2Sb_2Te_5$. In addition, surface crystallization was not observed at this initial stage of phase transformation (below the inflection point).

Next, we compared the structure of the GST films annealed at 168 ºC with exposure for 30 minutes and 183 ºC without exposure. It can be seen from Fig. 4a that in both cases the resistivity decreases to a similar value corresponding to the end of the GST phase transition from an amorphous to a metastable crystalline state. Electron diffraction analysis shows that both films have a polycrystalline structure (Fig. 4b,e). The average grain sizes were estimated on the basis of the experimental radial intensity profiles (Fig. 4d) according to the Scherrer formula and were equal about 10 nm. In order to perform a more detailed analysis of the grain size, bright-field TEM images obtained using an objective aperture of 10 μm were used (Fig. 4c,f). It was found that as the distance from the $SiO_2$/GST interface increases, the grain sizes grow from 4-6 to 25-30 nm. In both samples, the upper part of the film with a thickness of about 30 nm near the protective Pt layer deposited during TEM specimen preparation differs from the main part of the film. The grains in the upper part are significantly larger and have a columnar structure.

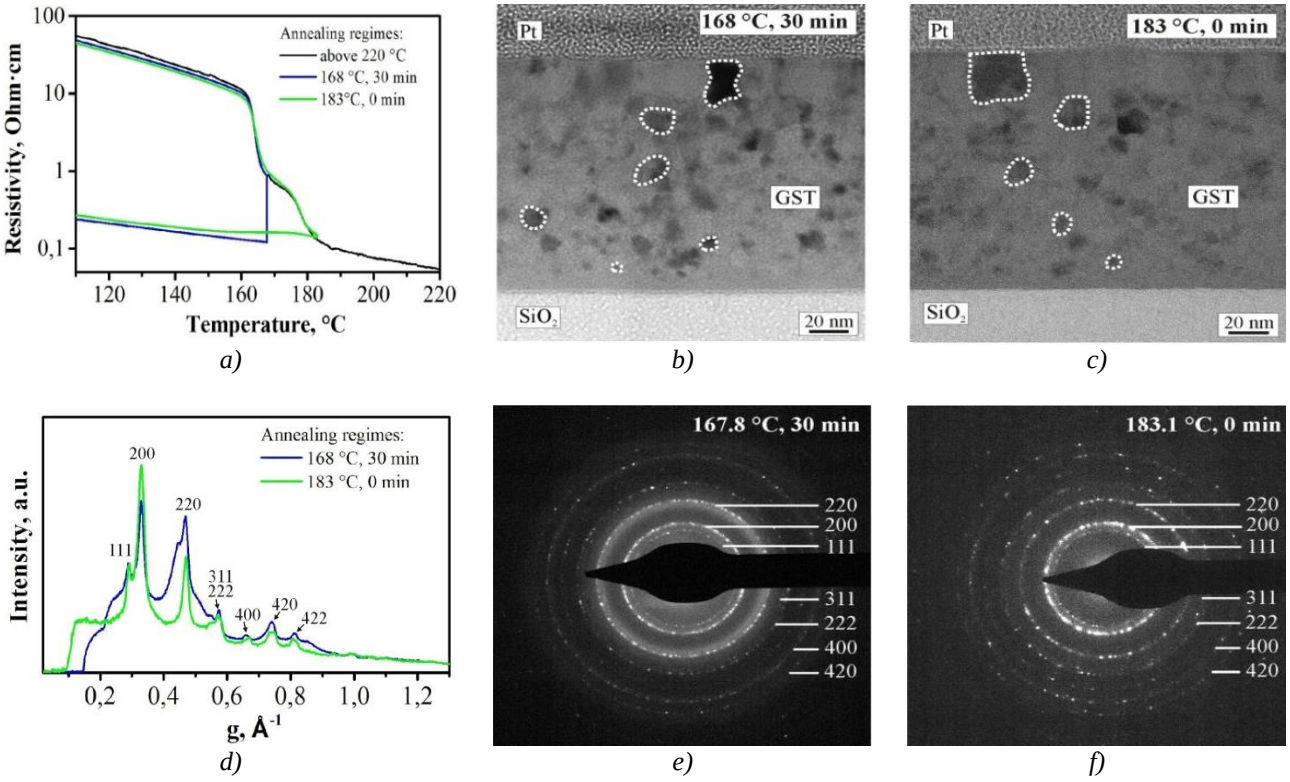


*Fig. 4. The temperature dependencies of resistivity for the investigated samples (a), bright-field TEM images (some crystalline areas are highlighted by dashed lines) and SAED patterns for the samples after annealing at 168 °C for 30 minutes (b,e) and 183 °C without exposure (c,f), radial intensity profiles formed on the basis of diffraction data (d)*

The fact that the mean size of crystalline grains and, therefore, their concentrations are practically the same for both considered samples, implies, that the growth of crystalline centers are the dominant process at this stage. In other words, no new crystalline nuclei emerge after the initial stage. However, it is evident that the number of grains in polycrystalline structure is greater than the number of crystallites observed in the sample heated to 168 °C without exposure. Due to strong temperature dependence of crystallization parameters of $Ge_2Sb_2Te_5$ it is unlikely that considerably different heating regimes (after the point 168 °C) can produce the polycrystalline structure of the similar parameters. This is why we believe that the final polycrystalline structure of the material is governed by the initial stage of crystallization before the inflection point. Because of the above mentioned difference between the number of crystallites observable after the initial crystallization stage and the concentration of the crystalline grains in the fully crystallized material we can assume, that not every centre of crystallization formed during the initial stage can be detected in our experiment. Small atomic rearrangements indistinguishable in the surrounding amorphous phase could lead to the local nucleation barrier lowering facilitating subsequent crystallization. These hidden changes could be also involved in the lowering of the material resistivity during the initial stage of crystallization. After all the nucleation centers were formed up to the inflection point, it does not matter what is the temperature profile that is used during subsequent annealing. Growth of crystallization centers eventually leads to the polycrystalline structure with the grains concentration determined by the initial stage of crystallization.

TEM images clearly show that the parameters of phase transition near both film boundaries are different in comparison with the volume and between each other. The latter, most probably, is attributed to the difference in the layers contacting with both film boundaries. It is known [29] that capping layers tend to increase the potential barrier for crystallization of phase change material films, comparing to the uncovered films. This could explain the amorphous layer at the film-substrate surface. On the other, free, film boundary, the opposite situation is observed -

crystalline grains are bigger, and the whole surface layer has a columnar structure. The reason for this could be the nucleation at the film surface. With such a nucleation mechanism, growth of crystallization centers should proceed from the film boundary forming columnar grains.

Therefore, the inflection point on the temperature dependence of $Ge_2Sb_2Te_5$ resistivity is the manifestation of an apparently two-stage character of the process of $Ge_2Sb_2Te_5$ thin films crystallization. During the first stage, the distribution of crystallization centers is formed. The second stage involves the growth of previously emerged centers without increasing their number.

## 4. Conclusions

We investigated $Ge_2Sb_2Te_5$ thin films annealed at the temperatures specific to the crystallization process using transmission electron microscopy. The temperatures typical for the inflection point (168 °C) of the curve and at the end of the crystallization process (183 °C) were chosen for the TEM studies. It was established that annealing at 168 °C leads to the nucleation of the small GST grains with fcc lattice, although in general the film structure remains amorphous. These results do not give reason to talk about the formation of conductive percolation channels. However, the resistance drops by more than an order of magnitude at the same time.

Upon further heating to 183 °C, a polycrystalline GST structure forms in the film. The crystalline grains in the upper part are significantly larger and have a columnar structure, while the thin amorphous layer (5-10 nm) was found at the film-substrate surface. Comparison of the films annealed at 183 °C and 168 °C with exposure for 30 minutes showed that in both cases the same GST structure is formed. So, the inflection point on the temperature dependence of Ge2Sb2Te5 resistivity could be the manifestation of an apparently two-stage character of the process of Ge2Sb2Te5 thin films crystallization. During the first stage, the distribution of crystallization centers is formed. The second stage involves the growth of previously emerged centers without increasing their number.

**Acknowledgements**

This study was supported by the Russian Federation President's grant (MK-6347.2018.3) and the Russian Foundation for Basic Research (project number 18-33-20237\18). The studies were performed using equipment of Core facilities centers "Diagnostics and modification of microstructures and nanoobjects", "MEMS and electronic components", and "STI Sensory" of MIET.

## References

[1] K. Shportko, S. Kremers, M. Woda, D. Lencer, J. Robertson, M. Wuttig Nature materials **7**(8), 653 (2008).
[2] M. Wuttig, N. Yamada, Nature materials **6**(11), 824 (2007).
[3] C. Rios, M. Stegmaier, P. Hosseini, D. Wang, T. Scherer, C.D. Wright, H. Bhaskaran, W. H. P. Pernice, Nature Photonics **9**(11), 725 (2015).
[4] S. Raoux, W. Welnic, D. Ielmini, Chemical reviews **110**, 240 (2010).
[5] Z. Guo, X. Yang, F. Shen, Q. Zhou, J. Gao, K. Guo, Scientific Reports **8**, 12433 (2018).
[6] P. Hosseini, C. D. Wright, H. Bhaskaran, Nature **511**, 206 (2014).
[7] S. G. Carillo, L. Trimby, Y. Au, V.K. Nagareddy, G. Rodriguez-Hernandez, P. Hosseini, C. Rios, H. Bhaskaran, C.D. Wright, Advanced optical materials, 801782 (2019).
[8] A. Redaelli, Phase change memory. Device physics, reliability and applications, Springer International Publishing (2018).
[9] Y. J. Park, J. Y. Lee, Y. T. Kim, Applied surface science **252**, 8102 (2006).
[10] Y. Zheng, Y. Cheng, R. Huang, R. Qi, F. Rao, K. Ding, W. Yin, S. Song, W. Liu, Z. Song, S. Feng, Scientific reports **7**(1), 5915 (2017).

[11] A. Lotnyk, T. Dankwort, I. Hilmi, L. Kienle, B. Rauschenbach, Nanoscale **11**, 10838 (2019).
[12] N. Yamada, T. Matsunaga, Journal of applied physics **88**(12), 7020 (2000).
[13] I. Friedrich, V. Weidenhof, Journal of applied physics **87**(9), 4130 (2000).
[14] J. Wang, Y. Xu, R. Mazzarello, M. Wuttig, W. Zhang, Materials **10**, 862 (2017).
[15] Q. Yin, L. Chen, Journal of Materials Science: Materials in Electronics **29**(19), 16523 (2018).
[16] C. Koch, A. L. Hansen, T. Dankwort, G. Schienke, M. Paulsen, D. Meyer, M. Wimmer, M. Wuttig, L. Kienle, W. Bensch, RSC Advances **7**(28), 17164 (2017).
[17] T. Li, L. Wu, X. Ji, Y. Zheng, G. Liu, Z. Song, J. Shi, M. Zhu, S. Song, S. Feng, AIP Advances **8**(2), 025201 (2018).
[18] P. Guo, G. A. Sevison, J. A. Burrow, I. Agha, A. Sarangan, Nanoengineering: Fabrication, Properties, Optics, and Devices XV **10730**, 107300L (2018).
[19] L. Cao, X. Ji, W. Zhu, Q. She, Y. Chen, Z. Hu, S. Guo, Z. Song, F. Rao, B. Qian, L. Wu, ECS Solid State Letters, **4**(12), 102 (2015).
[20] Y. Hu, R. Zhang, T. Lai, X. Zhu, H. Zou, Z. Song, ECS Journal of Solid State Science and Technology, **6**(12), 866 (2017).
[21] E. N. Voronkov, A. I. Popov, I. S. Savinov, A. R. Fairushin, Journal of Non-Crystalline Solids **352**, 1578 (2006).
[22] J. Mayer, L.A. Giannuzzi, T. Kamino, J. Michael, MRS bulletin **32**(5), 400 (2007).
[23] T. Nakaoka, H. Satoh, S. Honjo, H. Takeuchi, AIP Advances **2**, 042189 (2012).
[24] S. Privitera, E. Rimini, Journal of applied physics **94**(7), 4409 (2003).
[25] N. F. Mott, E. A. Davis, Electronic processes in non-crystalline materials, Oxford university press (2012).
[26] P. Lazarenko, M. Savelyev, A, Sherchenkov, A. Gerasimenko, S. Kozyukhin, V. Glukhenkaya, A. Polokhin, Y. Shaman, A. Vinogradov, Chalcogenide letters **15**(1), 25 (2018).
[27] P. Guo, A. M. Sarangan, I. Agha, Applied sciences **9**(3), 530 (2019).
[28] V. D. A. G. Bruggeman, Annalen der physik **416**(7), 636 (1935).
[29] N. Ohsima, Journal of applied physics **79**(11), 8357 (1996).